MECHANICS RESEARCH COMMUNICATIONS Vol. 17 (2), 81-91, 1990. Printed in the USA.
0093-6413/90 $3.00 + .00

AN ADAPTIVE MESH REFINEMENT TECHNIQUE FOR THE ANALYSIS OF ADIABATIC SHEAR BANDING

R. C. Batra and C. H. Kim
Department of Mechanical and Aerospace Engineering and
Engineering Mechanics, University of Missouri-Rolla,
Rolla, MO 65401-0249

(Received 30 June1989; accepted for print 5 December 1989)

Abstract

Adiabatic shear bands are narrow regions in which the shear strain is several orders of magnitude higher than that in the adjoining regions. Because of the steep gradients of deformation within and near these bands, a properly graded mesh is required for a satisfactory resolution of the details of the deformation field. Here we use the scaled residuals in the equations expressing the balance of linear momentum and the balance of internal energy to refine the mesh adaptively. The computed results show that the two balance laws generally require refinement of the mesh in different regions.

1. Introduction

Adiabatic shear banding refers to the localization phenomenon that occurs during many high-rate plastic deformation processes such as machining, shock impact loading, ballistic penetration, and metal forming. As shear bands are believed to be precursors to material fracture, a knowledge of factors that inhibit or enhance their initiation and growth, is essential to the production of durable materials and the design of optimum processing environment and conditions.

The interest in adiabatic shear banding seems to have started with the work of Zener and Hollomon[1] who observed 32 μm wide shear bands in a steel plate punched by a standard die and estimated the maximum strain in the band to be 100. Analytical studies aimed at finding critical conditions necessary for the initiation and growth of adiabatic shear bands include the work of Clifton[2], Bai[3], Staker[4], Burns[5], Anand et al.[6], and Wright[7]. Experimental investigations have been carried out, among others, by Costin et al.[8], Moss[9], Lindholm and Johnson[10], and Marchand and Duffy[11]. Of these, Marchand and Duffy[11] have provided a detailed history of the temperature and strain field during the initiation and development of a shear band. Numerical computations of Clifton et al.[12], Wright and Batra[13], Wright and Walter[14], Batra[15], and Batra and Kim[16] have revealed some interesting aspects of adiabatic shear banding. Whereas these investigations involved analyzing simple shearing deformations of a viscoplastic block, recently, Needleman[17], and Batra and Liu[18] studied the initiation of shear bands in plane-strain

deformations of viscoplastic solids. All of the numerical studies referred to above have used a fixed finite element or finite difference mesh. In general, the computed results depend upon the mesh used. Needleman[19] has discussed this aspect in considerable detail. A robust code should have a properly graded mesh and should be able to compute results with the least usage of the CPU time.

Drew and Flaherty[20] have used the moving grid method to develop an adaptive finite element code that automatically locates regions with large gradients and concentrates finite elements there in order to minimize approximately the discretization error per time step. Pervaiz and Baron[21] have discussed an adaptive technique which refines the spatial and/or temporal grid whenever preselected gradients exceed the threshold levels and have applied it to study quasi-one-dimensional unsteady flow problems involving finite rate chemistry. Herein we use the local refinement method to develop an adaptive mesh refinement technique that makes the scaled residuals uniformly distributed within the domain. The technique is applied to study the simple shearing deformations of a viscoplastic block whose material exhibits strain and strain-rate hardening and thermal softening. Results computed with a fixed mesh and an adaptively refined mesh differ quantitatively only after the deformations have started to localize. Also it is found that the residuals in the balance of the linear momentum and the balance of internal energy are generally not high in the same region. Thus different regions need to be refined to lower the residuals in the two equations.

2. Governing Equations

Equations governing the overall adiabatic thermomechanical deformations of a viscoplastic block bounded within the planes $y = \pm 1$ and undergoing simple shearing deformations are[13,15]

$$\dot{v} = (1/\rho)\, s_{,y}, \tag{2.1}$$

$$\dot{\theta} = k\theta_{,yy} + s\dot{\gamma}_p , \tag{2.2}$$

$$\dot{s} = \mu(v_{,y} - \dot{\gamma}_p) , \tag{2.3}$$

$$\dot{\psi} = s\dot{\gamma}_p/(1 + \psi/\psi_o)^n , \tag{2.4}$$

$$\dot{\gamma}_p = \max\left[0, \frac{1}{b}\left(\left(\frac{s}{(1 + \frac{\psi}{\psi_o})^n(1 - \alpha\theta)}\right)^{1/m} - 1\right)\right] , \tag{2.5}$$

with boundary conditions

$$v(\pm 1, t) = \pm 1 , \quad \theta_{,y}(\pm 1, t) = 0 \tag{2.6}$$

and a suitable set of initial conditions. These equations are

written in terms of nondimensional variables related to their dimensional counterparts, indicated below by a superimposed bar, as follows:

$$y = \bar{y}/H,\ v = \bar{v}/v_o,\ t = \bar{t}\ v_o/H,\ s = \bar{s}/s_o\ ,$$

$$\theta = \bar{\theta}/\theta_o,\ \theta_o = s_o/\bar{\rho}c,\ \rho = \bar{\rho}\ v_o^2/s_o,\ k = \bar{k}/(\bar{\rho}cv_oH)\ , \tag{2.7}$$

$$\psi = \bar{\psi}\ ,\ \alpha = \bar{\alpha}\theta_o,\ b = \bar{b}\ v_o/H.$$

Here v_o is the velocity imposed on the top and bottom surfaces of the block of height 2H and s_o is the flow stress in a quasistatic simple shear test. Equations (2.1) and (2.2) express, respectively, the balance of linear momentum and the balance of internal energy. In these equations ρ is the mass density, θ the temperature change of a material particle from that in the reference configuration, k the thermal diffusivity, γ_p the plastic strain-rate, μ the shear modulus, ψ_o and n characterize the work hardening of the material, parameters b and m describe its strain-rate hardening and α the thermal softening. Furthermore, a superimposed dot indicates the material time derivative and a comma followed by y stands for partial differentiation with respect to y. In writing eqn. (2.3) we have assumed that the strain-rate γ has an additive decomposition into elastic γ_e and plastic parts γ_p, i.e.

$$\dot{\gamma} = \dot{\gamma}_e + \dot{\gamma}_p. \tag{2.8}$$

The internal variable ψ rather than the plastic strain γ_p is used to describe the work-hardening of the material and accounts approximately for the history of the deformation. The rate of evolution of ψ is assumed to be given by equation (2.4). Equation (2.5) states that the plastic strain-rate vanishes whenever

$$s \le (1 + \frac{\psi}{\psi_o})^n(1 - \alpha\theta); \tag{2.9}$$

otherwise it is computed by solving the equation

$$s = (1 + \frac{\psi}{\psi_o})^n(1 - \alpha\theta)\ (1 + b\ \dot{\gamma}_p)^m \tag{2.10}$$

which is a slight generalization of the Litonski equation. A detailed discussion of constitutive assumptions (2.4), (2.5), (2.9) and (2.10) is given in Refs. 13 and 16. The boundary conditions (2.6) imply that the body is placed in a hard perfectly insulated loading device in the sense that the tangential velocity is prescribed on its top and bottom faces which do not exchange heat with their surroundings.

For the initial conditions we take

$$v(y,0) = y,\ \psi(y,0) = 0\ ,$$

$$\theta(y,0) = 0.1 + 0.1\ (1 - y^2)^9\ \exp(-5y^2), \qquad (2.11)$$

$$s(y,0) = (1 - \alpha\theta(y,0))(1+b)^m\ ,$$

and seek solutions which exhibit the properties

$$v(-y,t) = -v(y,t),\ s(-y,t) = s(y,t),\ \theta(-y,t) = \theta(y,t)\ . \qquad (2.12)$$

Thus the problem needs to be solved on the domain $0 \leq y \leq 1$ with the boundary conditions (2.6) replaced by

$$v(1,t) = 1,\ \theta_{,y}(1,t) = 0,\ v(0,t) = 0,\ \theta_{,y}(0,t) = 0\ . \qquad (2.13)$$

The initial conditions (2.11) imply that the transients have died out. The second term on the right-hand side of $(2.11)_2$ gives the temperature perturbation which simulates a material inhomogeneity or defect in the body. The size and shape of the temperature perturbation is supposed to model the strength and distribution of the material defect. The final width of the shear band should not depend upon the assumed form of $(2.11)_2$ which was also used in Refs. 13-16. The body is initially taken to be heated to a temperature of 0.10 to reduce the CPU time required to solve the problem. Our aim here is to see how the residuals in the balance of linear momentum and balance of internal energy are distributed, refine the mesh accordingly, and see if the mesh refinements lead to superior results.

We use Galerkin's approximation[22] and piecewise linear finite element basis functions to derive a semi-discrete formulation of the problem defined by equations (2.1) - (2.5), (2.11) and (2.12), and the Crank-Nicolson method to integrate the resulting nonlinear coupled ordinary differential equations. The details of obtaining the nonlinear algebraic equations from (2.1) - (2.5), (2.11) and (2.12) are given in Ref. 15.

3. An Adaptive Mesh Refinement Technique

We employ the method of scaled residuals, similar to that outlined by Carey and Oden[23], to selectively refine the mesh in appropriate subregions of the domain. Thus it is tacitly assumed that a large scaled residual in a subregion implies that the solution is inaccurate there. Other refinement criteria such as the gradient of a solution variable exceeding a preassigned value could have been employed. What is the most appropriate rule for the problem at hand is an open question. No *a priori* estimates are available because of the strong nonlinearities present in the problem. We have used the following procedure to refine the mesh adaptively in the spatial domain.

1. Define an initial mesh M^o and find an approximate solution of equations (2.1) - (2.6) and (2.11) until the time the mesh is to be checked for possible refinement.

2. Using the solution computed in step 1, calculate the scaled element residual

$$R_\alpha^e = \frac{1}{\ell_e} \left(\int_{\Omega_e} r_\alpha^2 \, dy \right)^{1/2} , \quad \alpha = 1,2 . \tag{3.1}$$

Here ℓ_e is the length of element Ω_e, and

$$r_1 = \dot{v}^h - \frac{1}{\rho} s^h{}_{,y} , \tag{3.2}$$

$$r_2 = \dot{\theta}^h - k \, \theta^h{}_{,yy} - s^h \dot{\gamma}^h_p , \tag{3.3}$$

the superscript h indicates that the corresponding field variable is computed from the approximate solution. We note that r_1 and r_2 equal, respectively, the errors in satisfying the balance of linear momentum and the balance of internal energy. We have used 4-point Gauss quadrature rule to evaluate numerically the integral in equation (3.1).

3. Find the mean $\bar{R}_\alpha$ (M^o) and the standard deviation σ_α (M^o) of the set

$\{R_\alpha^e\}$ of scaled element residuals.

4. Cycle over the elements. If in an element either

$$C_1 = (R_1^e - \bar{R}_1)/\sigma_1 \geq 1.0 , \tag{3.4}$$

or

$$C_2 = (R_2^e - R_2)/\sigma_2 \geq 1.0 , \tag{3.5}$$

subdivide the element into two equal elements. At the newly introduced nodes the variables are assigned values obtained by linear interpolation of the solution computed in step 1.

5. The mesh M^o is replaced by this new mesh, and we repeat steps 1 through 4.

4. Results for a Sample Problem

We illustrate the aforementioned adaptive mesh refinement tech-

nique by computing results for a sample problem and assign values to various material and geometric parameters as follows:

$$\rho = 3.928 \times 10^{-5},\ k = 3.978 \times 10^{-3},\ \mu = 240.3,\ m = 0.025, \qquad (4.1)$$

$$n = 0.09,\ \psi_o = 0.017,\ \alpha = 0.4973,\ b = 5 \times 10^{6},\ \dot{\gamma}_o \equiv v_o/H = 500\ \text{sec}^{-1}.$$

These values, except for α, are for a typical steel. We chose a rather high value for α, equal to seven times that for a typical steel, to cut down on the CPU time required to solve the problem. Not knowing in advance at what values of time t to refine the mesh, we tried the following three alternatives:

1. Refine the mesh at t = 2 μs, 20 μs, 40 μs, 60 μs, 80 μs, 100 μs, 120 μs, 140 μs, 160 μs, and 180 μs.

2. Refine the mesh at t = 2 μs, 70 μs, 80 μs, 90 μs, 100 μs, 110 μs, 120 μs, 130 μs, 155 μs, and 180 μs.

3. Refine the mesh at t = 2 μs, 60 μs, 120 μs, 130 μs, 140 μs, 150 μs, 160 μs, 170 μs, 180 μs, and 185 μs.

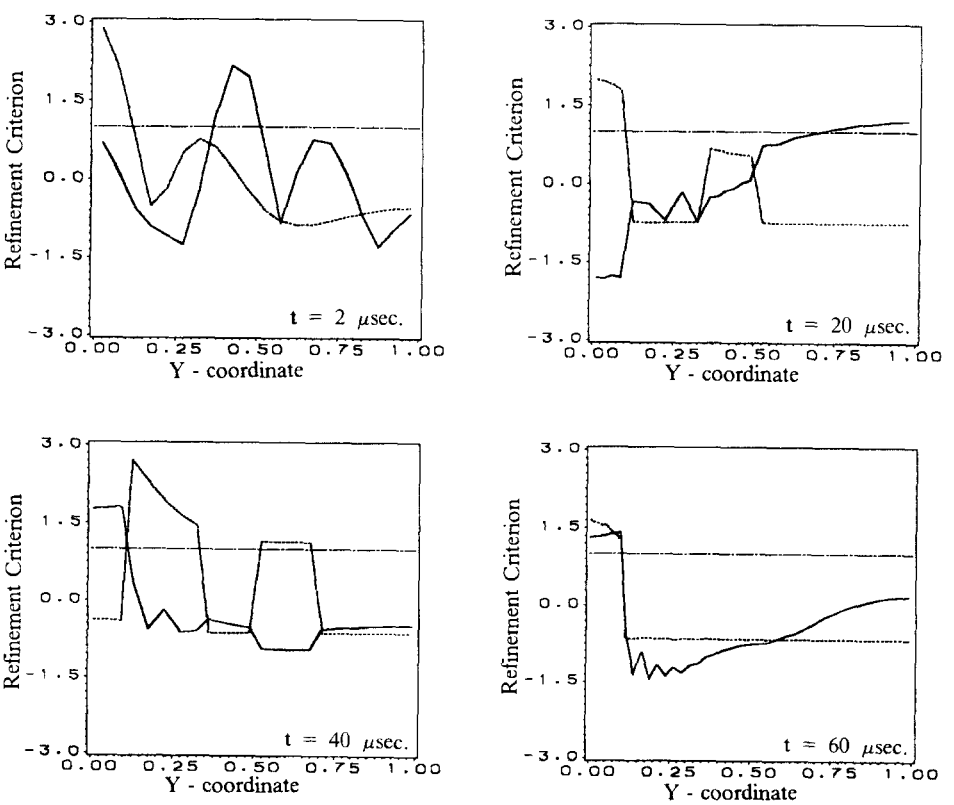

Figure 1. Distribution of the refinement criterion C_1 and C_2 at t = 2 μs, 20 μs, 40 μs and 60 μs. (Solid Line: Linear Momentum; Dotted Line: Internal Energy)

For each one of these choices, different meshes were computed for t = 140 μs but the results were virtually indistinguishable up to and including t = 140 μs. Also the deformation had localized prior to the next refinement of the mesh. We took the solution at t = 120 μs as the initial data and restarted the job with the mesh to be refined at every 4 μs interval until t = 140 μs. The mesh was not refined subsequently. The initial mesh at t = 0 had 20 uniform elements. The final mesh at t = 140 μs had 458 non-uniform elements of which 423 were located between 0 and 0.10.

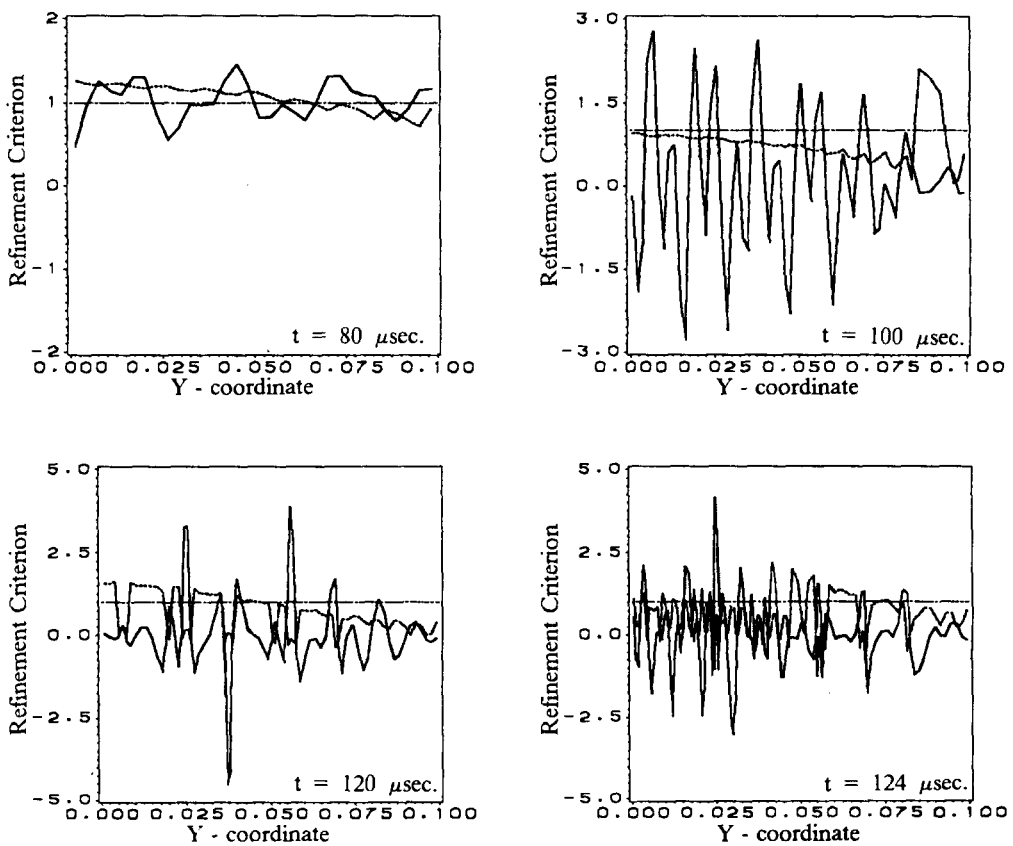

Figure 2. Distribution of the refinement criterion C_1 and C_2 at t = 80 μs, 100 μs, 120 μs, 124 μs. (Solid Line: Linear Momentum; Dotted Line: Internal Energy)

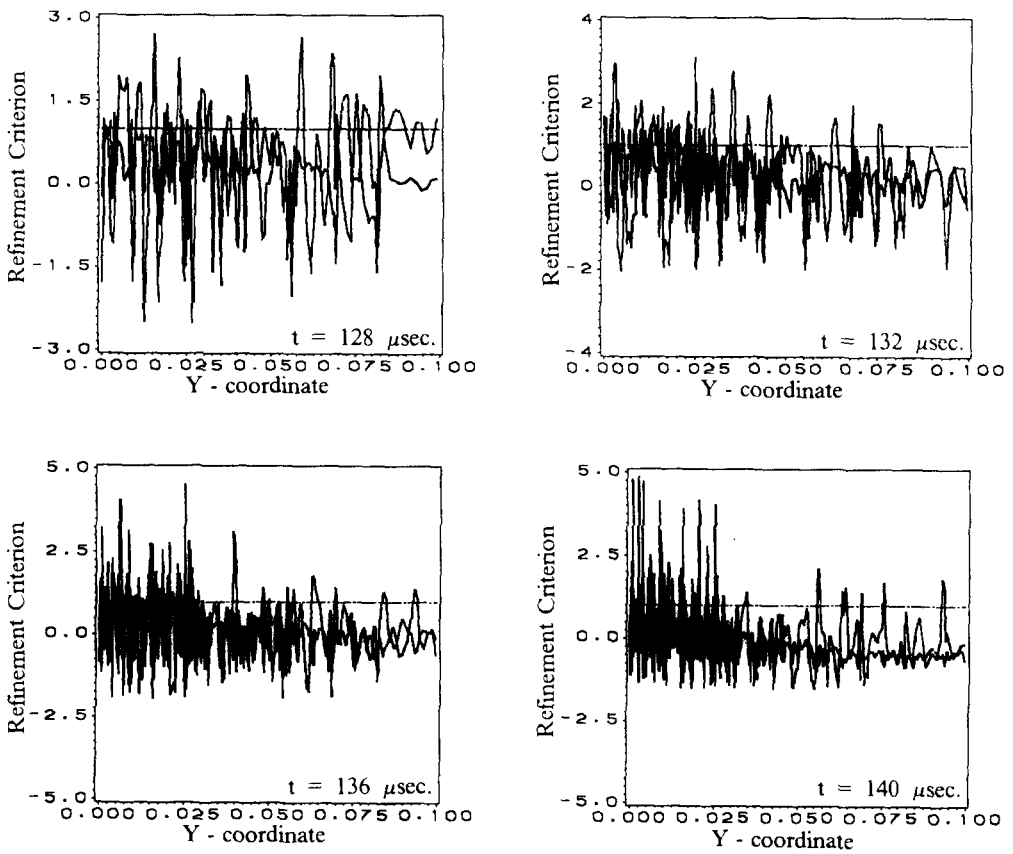

Figure 3. Distribution of the refinement criterion C_1 and C_2 at t = 128 μs, 132 μs, 136 μs, 140 μs. (Solid Line: Linear Momentum; Dotted Line: Internal Energy)

Figure 1 depicts the distribution of the refinement criteria C_1 and C_2 at t = 2 μs, 20 μs, 40 μs and 60 μs. Initially the distribution of scaled residuals in equations expressing the balance of linear momentum and the balance of internal energy require refinement of the mesh in different regions. However, for $t \geq 60$ μs the scaled residuals in both equations are relatively high only near the center of the block. Thus, we have plotted in Figures 2 and 3 the distribution of C_1 and C_2 within $0 \leq y \leq 0.10$ at t = 80 μs, 100 μs, 120 μs, 124 μs, 128 μs, 132 μs, 136 μs and 140 μs. The values of C_1 and C_2 were less than 1.0 for $y > 0.10$ at the discrete values of t listed in the preceding sentence. For t = 80 μs, 100 μs, 120 μs and 124 μs C_2 varies smoothly and its magnitude does not change a great deal. Starting at t = 100 μs the values of C_1 oscillate quite a bit but are generally less than 1.0. This may be an indication of the initiation of the localization of the deformation. At t = 128 μs, 132 μs, 136 μs and 140 μs, the region where C_1 and C_2 undergo severe oscillations progressively narrows down to that near y = 0. At t = 136 μs and 140 μs both C_1 and C_2 are generally less than 1.0 for $y \geq$

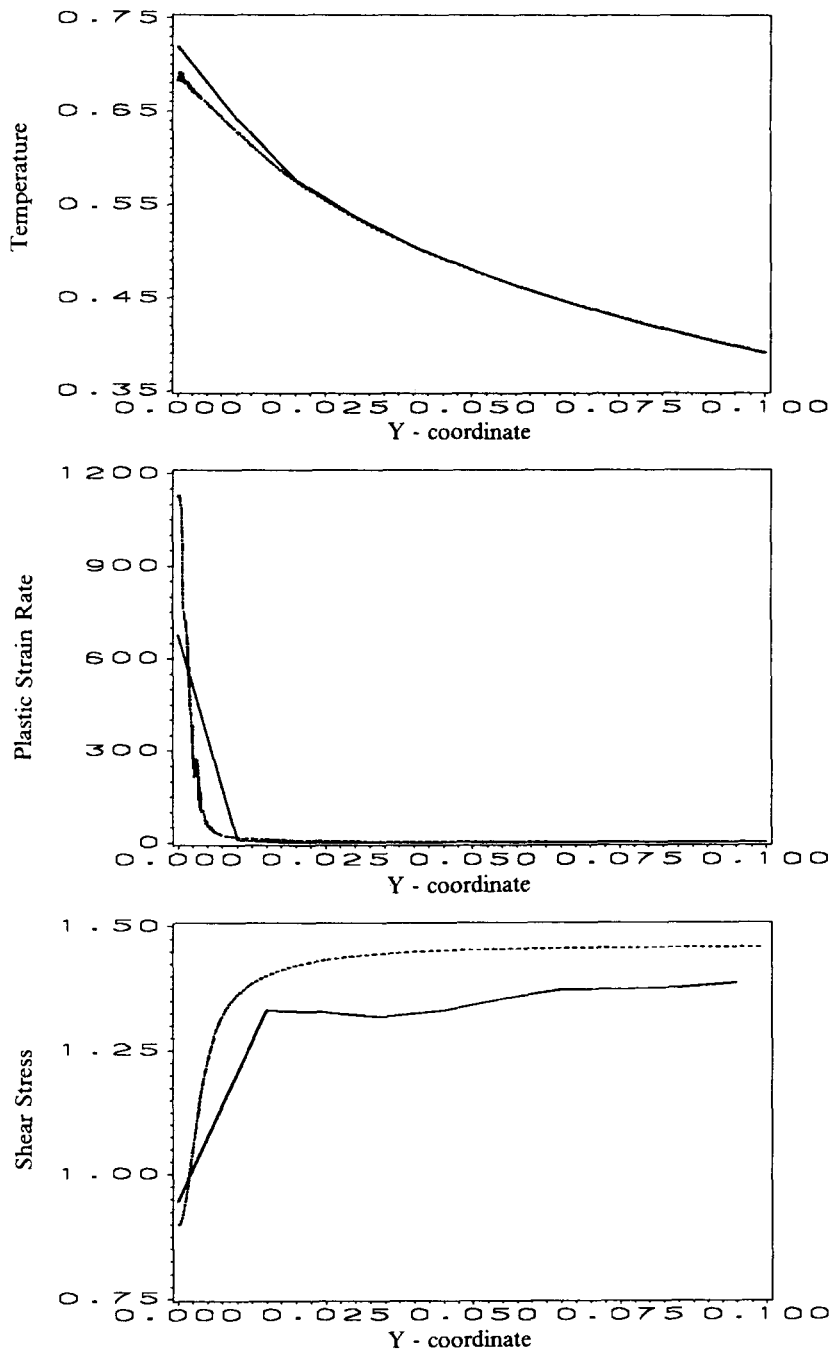

Figure 4. Spatial distribution of the temperature, shear stress and plastic strain at $\gamma_{avg} = 0.142$. (Solid Line: Uniform Mesh; Dotted Line: Refined Mesh)

0.025 implying thereby that some of the nodes could possibly be removed from this region. We are now in the process of adding to our code the capability to combine two or more elements into one and dividing one element into two or more elements depending upon the magnitude and sign of $(C_1 - 1.0)$ and $(C_2 - 1.0)$.

In order to see the improvement, if any, in the results computed with a mesh refined adaptively as compared to those computed with a uniform 100-element mesh we have plotted in Fig. 4 the spatial variation of the temperature, plastic strain-rate and the shear stress. These results confirm the expectation that the adaptively refined mesh can resolve sharp gradients of the deformation fields within the region of localization. From the distribution of the plastic strain-rate it is transparent that the width of the shear band as computed from the adaptively refined mesh is very small as compared to that with the uniform mesh. With the latter mesh it equals the size of one element clearly indicating that the mesh is too coarse. Also with the uniform mesh the oscillations in the value of the shear stress from node to node were very large as compared to those with the adaptively refined mesh. The data plotted represents the average of the values at two consecutive nodes. These oscillations in the shear stress are probably due to the propagation of an unloading elastic shear wave out of the region of localization. The propagation of the wave is not clearly resolved because of the time integration scheme used herein.

5. Discussion and Conclusions

The use of an adaptive mesh refinement technique based on distributing the scaled residuals uniformly throughout the domain for solving the adiabatic shear band problem has enabled us to resolve adequately the sharp gradients of the deformation field within the region of localization. Initially, refinements of the mesh are required by the scaled residuals in the equations expressing the balance of internal energy and the balance of linear momentum. As the deformation begins to localize near the center of the block, the scaled residuals in the energy equation stay essentially equally distributed except when the localization is in progress earnestly. However, the scaled residuals in the linear momentum equation oscillate and do necessitate the refinement of the mesh in several regions.

The computed results indicate that the mesh can be refined less frequently prior to the onset of the localization but ought to be refined very frequently subsequent to the initiation of the localization of the deformation. We are now working on the adaptive refinement of the mesh in the time domain.

Acknowledgements: This work was supported by the U.S. National Science Foundation grant MSM-8715952, the U.S. Army Research Office Contract DAAL 03-88-K-0184, and the University of Missouri Weldon Spring Fund.

REFERENCES

1. C. Zener and J. H. Hollomon, J. Appl. Phys., 14, 22-32 (1944).
2. R. J. Clifton, U.S. NRC National Material Advisory Board Report NMAB-356, Herman, W., et al. eds. (1980).
3. Y. L. Bai, In: Shock Waves and High Strain - Rate Phenomena in Metals, Meyers, M. A., and Murr, L. E., eds., Plenum Press, New York (1981).
4. M. R. Staker, Acta Metall., 29, 683 (1981).
5. T. J. Burns, Q. Appl. Math., 43, 65-84 (1985).
6. L. Anand, K. H. Kim, and T. G. Shawki, J. Mechs. Phys. Solids, 35, 407-429 (1987).
7. T. W. Wright, J. Mechs. Phys. Solids, 35, 269-282 (1987).
8. L. S. Costin, E. E. Crisman, R. H. Hawley, and J. Duffy, Inst. Phys. Conf. Ser., 47, 90-100 (1979).
9. G. L. Moss, In: Shock Waves and High Strain-Rate Phenomenon in Metals, Meyers, M. A. and Murr, L. E., eds., Plenum Press, New York, pp. 299-312 (1981).
10. U. S. Lindholm and G. R. Johnson, In: Material Behavior Under High Stresses and Ultrahigh Loading Rates, Mescal, J. and Weiss, V., eds., 61-79 (1983).
11. A. Marchand and J. Duffy, J. Mech. Phys. Solids, 36, 251-283 (1988).
12. R. J. Clifton, J. Duffy, K. A. Hartley, and T. G. Shawki, Scripta Metall., 18, 443 - 448 (1984).
13. T. W. Wright and R. C. Batra, Int. J. Plasticity, 1, 205-212 (1985).
14. T. W. Wright and J. Walter, J. Mech. Phys. Solids, 35, 701-716 (1987).
15. R. C. Batra, Int. J. Plasticity, 3, 75-89 (1987).
16. R. C. Batra, and C. H. Kim, Int. J. Plasticity, (in press).
17. A. Needleman, J. Appl. Mechs., 56, 1-9 (1989).
18. R. C. Batra and De-Shin Liu, J. Appl. Mechs., 56, 527-534 (1989).
19. A. Needleman, Comp. Meth. Appl. Mech. Eng., 67, 69-85 (1988).
20. D. A. Drew and J. E. Flaherty, In: Phase Transformations and Material Instabilities in Solids, M. E. Gurtin, ed., Academic Press, pp. 37-60 (1984).
21. M. M. Pervaiz and J. R. Baron, Comm. Appl. Num. Meth., 4, 97-111 (1988).
22. T. J. R. Hughes, The Finite Element Method. Linear Static and Dynamic Finite Element Analysis, Prentice Hall, Englewood Cliffs (1987).
23. G. F. Carey and J. T. Oden, Finite Elements. Computational Aspects, Vol. 3, Prentice Hall, Englewood Cliffs (1984).